

Investigating the High- And Low-Temperature Performance of Warm Crumb Rubber-Modified Bituminous Binders Using Rheological Tests

Wang, Haopeng; Liu, Xueyan; Apostolidis, Panos; Wang, Di; Leng, Zhen; Lu, Guoyang; Erkens, Sandra; Skarpas, Athanasios

DOI

[10.1061/JPEODX.0000326](https://doi.org/10.1061/JPEODX.0000326)

Publication date

2021

Document Version

Accepted author manuscript

Published in

Journal of Transportation Engineering Part B: Pavements

Citation (APA)

Wang, H., Liu, X., Apostolidis, P., Wang, D., Leng, Z., Lu, G., Erkens, S., & Skarpas, A. (2021). Investigating the High- And Low-Temperature Performance of Warm Crumb Rubber-Modified Bituminous Binders Using Rheological Tests. *Journal of Transportation Engineering Part B: Pavements*, 147(4), Article 04021067. <https://doi.org/10.1061/JPEODX.0000326>

Important note

To cite this publication, please use the final published version (if applicable). Please check the document version above.

Copyright

Other than for strictly personal use, it is not permitted to download, forward or distribute the text or part of it, without the consent of the author(s) and/or copyright holder(s), unless the work is under an open content license such as Creative Commons.

Takedown policy

Please contact us and provide details if you believe this document breaches copyrights. We will remove access to the work immediately and investigate your claim.

Investigating the High- and Low-temperature Performance of Warm Crumb Rubber Modified Bituminous Binders using Rheological Tests

Haopeng Wang, Ph.D. candidate

Section of Pavement Engineering, Faculty of Civil Engineering & Geosciences, Delft University of Technology, Stevinweg 1, 2628 CN, Delft, The Netherlands;

Department of Civil and Environmental Engineering, The Hong Kong Polytechnic University, Hong Kong, China.

Email: haopeng.wang@tudelft.nl

Xueyan Liu, Ph.D., Associate professor

Section of Pavement Engineering, Faculty of Civil Engineering & Geosciences, Delft University of Technology, Stevinweg 1, 2628 CN, Delft, The Netherlands

Panos Apostolidis, Ph.D. candidate

Section of Pavement Engineering, Faculty of Civil Engineering & Geosciences, Delft University of Technology, Stevinweg 1, 2628 CN, The Netherlands

Di Wang, Postdoctoral researcher

Department of Civil Engineering - ISBS, Technical University of Braunschweig, Braunschweig, Germany

Zhen Leng, Ph.D., Associate professor

Department of Civil and Environmental Engineering, The Hong Kong Polytechnic University, Hong Kong, China

Guoyang Lu, Ph.D., Research assistant professor (Corresponding author)

Department of Civil and Environmental Engineering, The Hong Kong Polytechnic University, Hong Kong, China

Sandra Erkens, Ph.D., Professor

Section of Pavement Engineering, Faculty of Civil Engineering & Geosciences, Delft University of Technology, Stevinweg 1, 2628 CN, The Netherlands

Athanasios Skarpas, Ph.D., Professor

Department of Civil Infrastructure and Environmental Engineering, Khalifa University, Abu Dhabi, United Arab Emirates;

Section of Pavement Engineering, Faculty of Civil Engineering & Geosciences, Delft University of Technology, Stevinweg 1, 2628 CN, The Netherlands

43 **ABSTRACT**

44 Rubberized asphaltic materials have been frequently combined with warm mix asphalt technologies to
45 tackle the issues of high energy consumptions and emissions during construction. Effective and accurate
46 characterization of binder properties is conducive to the improvement of long-term pavement
47 performance. The current study aims to quantify the effects of rubber content and warm-mix additives on
48 rutting and thermal cracking performance of crumb rubber modified bitumen (CRMB), and explore the
49 rubber and additives modification mechanisms and their impacts on the binder performance. CRMBs
50 containing different rubber contents and warm-mix additives after long-term aging were subject to
51 multiple stress creep and recovery (MSCR) tests and low-temperature frequency sweep tests using a
52 dynamic shear rheometer (DSR) with the 4-mm loading plate, to investigate the high- and low-
53 temperature performance, respectively. Rheological tests were also conducted on the bitumen and rubber
54 phases of CRMB to understand the rubber modification mechanism. Results show that CRMB binders
55 have superior rutting and thermal cracking resistance due to rubber modification. The improvement of
56 high- or low-temperature performance is more prominent at higher rubber concentrations. The effects of
57 warm-mix additives on the rutting and thermal cracking performance are different. Generally, the wax-
58 based additive improves the rutting resistance but negatively affects the low-temperature performance. By
59 contrast, the chemical-based additive has an opposite effect except for the high-temperature performance
60 of neat bitumen. The stiffening of the bitumen phase and the contribution of swollen rubber particles in the
61 bitumen matrix together contribute to the peculiar viscoelastic response of CRMB, i.e., stiffer/softer and
62 more elastic at high/low temperatures. This modification mechanism explains the superior rutting and
63 thermal cracking performance of CRMB.

64
65 *Keywords:* Bitumen, Crumb rubber, Warm-mix additives, Rutting, Thermal cracking, Rheology

66
67
68
69

70 INTRODUCTION

71 Crumb Rubber Modified Bitumen

72 Bitumen modification using crumb rubber from scrap tires has been increasingly popular in the context of
73 circular economy (Leng et al. 2018; Nanjegowda and Biligiri 2020). Although crumb rubber modified
74 bitumen (CRMB) has been reported to improve the engineering properties of binders (Singh et al. 2017;
75 Wang et al. 2018), its high viscosity has caused some concerns during construction, such as poor
76 pumpability, mixability, and workability (Wang et al. 2018; Yu et al. 2018). Besides, the requirement of
77 higher production temperatures of rubberized asphalt mixtures increases the heat energy consumption and
78 greenhouse gas emissions and generates more asphalt fumes, which compromises the working conditions
79 of paving crews at the construction site (Farshidi et al. 2013). The emergence of warm mix asphalt
80 (WMA) technologies provides an effective solution to the above issues by decreasing the construction
81 temperatures of rubberized asphalt (Wang et al. 2018; Yu et al. 2017). Since the combination of CRMB
82 with WMA is a relatively new implementation in the sustainable asphalt paving industry, it is important to
83 elucidate its long-term performance characteristics either in the laboratory or in the field.

84 Permanent deformation, fatigue, and thermal cracking are the primary distress modes of asphalt
85 pavements. Past research has demonstrated that the performance-related properties of the bituminous
86 phase has predominant effects on the durability of asphalt mixture (Bahia et al. 2001). The effective and
87 accurate characterization of binder performance is of great importance from the point of view of its
88 potential applications (Hajj and Bhasin 2017): (a) as a binder grading tool for design specification; (b) as a
89 screening/ranking tool to examine the influence of modifiers and additives; (c) to obtain fundamental
90 material properties of binders to be used as model inputs to predict the mechanical performance of
91 bituminous mixtures. Past studies have looked into the effects of rubber modification and various WMA
92 additives on the rutting and thermal cracking performance of CRMB binders through traditional test
93 methods and parameters (Daly and Negulescu 1997; Kim et al. 2010; Sebaaly et al. 2003; Singh et al.
94 2017). It was generally reported that rubber modification can improve the binders' resistance to permanent

95 deformation after long-term aging. Although rubber modification has been seen to improve the low-
96 temperature performance of binders, cautions need to be taken to properly design the CRMB, e.g., size
97 and content of crumb rubber (Sebaaly et al. 2003). In terms of WMA additives, their effects on the
98 properties of CRMB vary with the type of used WMA additives. Organic additives and chemical additives
99 usually affect the rutting or thermal cracking performance of CRMB binders in a different manner
100 (Akisetty et al. 2009; Kim et al. 2014; Yu et al. 2016). Therefore, it is necessary to characterize the high-
101 and low-temperature performance of binders for specific material combinations.

102 The fatigue performance of warm CRMB has been systematically investigated in a previous study (Wang
103 et al. 2020). Usually, contradictory measures were taken to increase the resistance of binders to permanent
104 deformation and thermal cracking. Balancing the high- and low-temperature performance is a major
105 challenge to mitigate these distresses. The current study emphasizes characterizing high- and low-
106 temperature performance and exploring the mechanism of the rubber modification to optimize the binder
107 design and to extend the durability of rubberized asphalt pavements.

108 **Binder Characterization for Rutting**

109 Under repeated traffic loadings, the accumulated strain in the bituminous binder is regarded as the main
110 reason for the rutting of asphalt pavements. Different methods and criteria have been developed to
111 characterize the propensity of a binder to permanent deformation under periodic loading. The Superpave
112 performance grading (PG) system uses the viscoelastic parameter ($G^*/\sin \delta$) measured from DSR as a
113 rutting parameter at high temperatures. The rutting parameter obtained in the linear viscoelastic range can
114 estimate the total dissipated energy during a loading cycle, which is believed to be related to rutting. To
115 minimize rutting, the energy dissipated per loading cycle should be minimized. Hence in a stress-
116 controlled test, the rutting parameter $G^*/\sin \delta$ should be maximized for binders at both fresh and short-
117 term aged states (Anderson and Kennedy 1993). However, many studies have demonstrated the
118 inadequacy of $G^*/\sin \delta$ in correlating with mixture rutting performance, especially for polymer modified
119 binders (Bahia et al. 2001). Attempts have been made to replace this inaccurate rutting parameter.

120 Sybilski (1994) proposed the concept of the zero-shear viscosity (ZSV) at 60 °C to characterize the
121 binder's rutting resistance. Good correlations between ZSV of binders and rutting performance of
122 mixtures were observed. However, other researchers found that highly polymer-modified binders, which
123 behave as viscoelastic solids, exhibit extremely high viscosity gradients at low shear rates, leading to
124 unrealistically high ZSV values using model predictions (De Visscher and Vanelstraete 2004).
125 Alternatively, the concept of low shear viscosity (LSV) was introduced to overcome this issue (Morea et
126 al. 2010).

127 Since the rutting parameter was obtained using small cyclic reversible loadings, the contribution of binder
128 damage accumulation was not considered. To address this, Bahia et al. (2001) developed the repeated
129 creep recovery (RCR) test using DSR to simulate the intermittent nature of traffic loading during the
130 NCHRP 9-10 project. The RCR test can separate the dissipated energy between permanent deformation
131 and delay elasticity. A novel parameter G_v derived from the Burger's model was introduced to
132 characterize the binder's resistance to permanent deformation. Considering the significant stress
133 dependency of polymer modified binders and different loading stress conditions, D'Angelo et al. (2007)
134 improved the RCR by introducing multiple stress creep and recovery (MSCR) tests. The MSCR is a
135 simple and performance-related test for both unmodified and modified binders. The non-recoverable
136 creep compliance (J_{nr}) and percent recovery were used to characterize the stress dependence and elastic
137 response of bituminous binders. Parameters from MSCR tests have been demonstrated to have a much
138 better correlation to mixture rutting performance than the existing Superpave binder criteria (D'Angelo
139 2009).

140 **Binder Characterization for Thermal Cracking**

141 Thermal cracking, including low-temperature shrinkage cracking and thermal fatigue cracking, is the
142 primary distress of asphalt pavements operating in cold regions such as northern American and northern
143 Europe. In Europe, most of the thermal cracking is low-temperature shrinkage cracking. With the decrease
144 of temperature, significant tensile stresses will develop in the asphalt surface layer and ultimately lead to

145 the initiation and propagation of cracks. As cracks mainly occur in the binder or mastic phase, it is vital to
146 select appropriate binders in mix design that satisfy the requirements of low-temperature performance
147 (Hajj et al. 2019). Many methods were proposed to evaluate the low-temperature properties of binders,
148 such as the Fraass breaking point test and low-temperature ductility test. However, these traditional tests
149 cannot accurately predict the critical temperature at which thermal cracking occurs (Wang et al. 2017).
150 The inadequacy is more significant when using these tests for the assessment of polymer modified binders
151 (Isacsson and Lu 1995).

152 The current Superpave PG system utilizes the bending beam rheometer (BBR) test to determine the low-
153 temperature PG of binders. Two parameters (i.e., creep stiffness and m -value (relaxation rate)) obtained
154 from the BBR test were used to determine the critical cracking temperature by applying two threshold
155 limits on them. The low-temperature PG of binders is ruled as the higher of below two values based on
156 two criteria: the temperature above which the maximum creep stiffness should not exceed 300 MPa and the
157 temperature above which the minimum m -value should not be less than 0.3. The creep stiffness is directly
158 related to the thermal stress built up in the bituminous material when temperature declines. Meanwhile,
159 the m -value shows the ability to retain the viscoelasticity and relaxing the accumulated thermal stress.

160 Standard BBR testing requires a relatively large amount of materials (15 g for each beam sample) which
161 may be inconvenient and difficult when assessing recovered binders or emulsion residues. Besides, BBR
162 tests often underestimate the low-temperature performance of polymer modified bitumen (PMB) (Lu et al.
163 2017). To overcome this limitation, researchers have explored the possibility of using a DSR with parallel
164 plates of 4 mm in diameter (4-mm DSR) as an alternative to the BBR (Farrar et al. 2015; Lu et al. 2017;
165 Oshone 2018; Sui et al. 2011; Wang et al. 2019). Besides the primary advantage of requiring a small
166 amount of binder, 4-mm DSR is a simple and more accurate method than BBR when measuring the low-
167 temperature rheological properties to determine the accumulated thermal stress (Farrar et al. 2013). It was
168 also reported that 4-mm DSR has good repeatability and good consistency among data collected from
169 different DSR plate sizes (Hajj et al. 2019; Sui et al. 2010).

170 **RESEARCH OBJECTIVES AND SCOPE**

171 The objectives of this study include: (1) to quantify the effects of rubber content and warm-mix additives
172 on rutting and thermal cracking performance of CRMB binders through new-generation rheological tests;
173 and (2) to explore the modification mechanism of rubber and additives for the binder performance. MSCR
174 tests were performed on the short-term aged binder samples to characterize the rutting performance. 4-mm
175 DSR frequency sweep (FS) tests were performed on the long-term aged binder samples to characterize the
176 thermal cracking performance. Furthermore, FS tests were also done on the bitumen and rubber phases of
177 CRMB to gain insights into the rubber modification mechanism and its impact on the overall binder
178 performance.

179 Together with a previous study on fatigue performance (Wang et al. 2020), this study is also part of the
180 attempt to characterize the binder properties in the whole temperature range (high-, intermediate- and low-
181 temperature) with only one DSR instrument using different plate sizes (25 mm, 8 mm, and 4 mm) as
182 shown in Figure 1. This unified DSR method is deemed to be a technical breakthrough enabling
183 improvements in the capacity of providing performance-related specifications for bituminous binders.

184 **MATERIALS AND METHODS**

185 **Raw Materials and Binder Sample Preparation**

186 Penetration grade 70/100 bitumen (Nynas) and fine CRMs from scrap truck tires (ambient grinding, size
187 ranging from 0 to 0.5 mm) were used to prepare CRMB binders. High shear mixer was applied to mix the
188 blend of neat bitumen and rubber of different percentages (5%, 10%, 15%, and 22% by weight of neat
189 bitumen) for 30 minutes at 180°C with a mixing speed of 6000 rpm. This mixing procedure was optimized
190 to allow sufficient rubber swelling to achieve optimized rheological properties (Wang et al. 2020). The
191 produced CRMBs were designated as CRMB-5, CRMB-10, CRMB-15, and CRMB-22. Two types of non-
192 foaming warm-mix additives, i.e., wax-based solid additive (W) and chemical-based liquid additive (C),
193 were added to neat bitumen and CRMB-22 at 160°C and mixed for 10 minutes. The resultant binders were
194 designated as 70/100-W, 70/100-C, CRMB-22-W, and CRMB-22-C. The reason why additives were only
195 added to CRMB-22 is that CRMB-22 exhibited extremely high viscosities, which will significantly

196 influence its pumpability, mixability, and workability if not reduced (Leng et al. 2017). The detailed
197 material properties and binder preparation process can be found in (Wang et al. 2020).

198 **Rotational Viscosity**

199 To examine the effect of rubber modification and warm-mix additives on the binder viscosity, the
200 Brookfield viscometer was used to measure the rotational viscosities of different binders at a constant
201 rotational speed of 20 rpm using the #27 cylindrical spindle (spindle diameter=11.76 mm, side
202 length=33.02 mm, effective length=39.29 mm). Viscosity tests were conducted at various temperatures,
203 110, 135, 160, 177, and 190°C, which cover the temperature range of production, transport, and
204 construction (Zhang et al. 2015).

205 Figure 2a shows the rotational viscosities of CRMB binders at various temperatures. It is obvious that
206 binder viscosity decreases with the increase of testing temperature. With the increase of rubber content,
207 the binder viscosity increases dramatically. Even at 190°C, the rotational viscosity of CRMB-22 has
208 exceeded 4000 mPa·s. Excessively high viscosities of CRMB will impede its application in asphalt
209 production and construction. Based on the recommended specification for rubberized bitumen in
210 California (State of California Department of Transportation 2003), the apparent viscosity of CRMB at
211 190°C should be in the range of 1500-4000 mPa·s to ensure the proper plant production. CRMB binders
212 with rubber contents lower than 15% have acceptable viscosities. Therefore, warm-mix additives need to
213 be incorporated into CRMB-22 to reduce the viscosity. Figure 2b shows the effect of warm-mix additives
214 on the viscosity of CRMB binders. For comparison, additives were also added to neat bitumen. As
215 expected, both additives effectively reduce the viscosity of both neat bitumen and CRMB. Particularly, the
216 viscosity of CRMB-22 has reduced to lower than 4000 mPa·s at 190 °C, which satisfies the specifications
217 for rubberized bitumen as proposed by Caltrans (California Department of Transportation). Therefore, for
218 the rest of the study, warm-mix additives were only added to CRMB-22 and neat bitumen for comparison
219 reason.

220 **Laboratory Ageing Procedure**

221 All fresh binder samples were short-term aged using oven aging as an alternative to the standard rolling
222 thin film oven (RTFO) test. This is because the RTFO ageing procedure encounters flowing and collecting
223 issues for highly viscous binders (e.g., CRMB) (Bahia et al. 1998). A modified oven aging procedure, in
224 which bitumen samples with a thickness of 1.25 mm were aged at 163°C for 2 h, was used to replace the
225 standard RTFO aging procedure in this study (Wang et al. 2020). A part of the short-term aged samples
226 were subject to MSCR tests. The remaining short-term aged samples were further aged by pressure aging
227 vessel (PAV) tests. The long-term aged samples were subject to 4-mm DSR tests.

228 **Preparation of Bitumen and Rubber Phases of CRMB**

229 In terms of bitumen and rubber phases of CRMB, considering the CRMB-22 binder as an example, the
230 bitumen phase of CRMB-22, which is designated as CRMB-22-BP, was extracted by filtering the
231 insoluble rubber particles from CRMB-22 with a mesh sieve (0.063-mm) at 163°C. The swollen rubber
232 samples were prepared to represent the rubber particle phase in CRMB. Cylindrical rubber samples (2-mm
233 in thickness and 8-mm in diameter) cut from waste truck tire tread were soaked in hot bitumen at 180°C to
234 prepare the swollen rubber samples. The detailed sample preparation process illustrated in Figure 3 can be
235 found in (Wang et al. 2020). Both CRMB-22-BP and swollen rubber samples were subject to FS tests by
236 DSR.

237 **MSCR Test Method**

238 The MSCR test was conducted using a DSR with 25-mm parallel plates AASHTO T 350-19. Considering
239 the weather conditions in the Netherlands, the maximum pavement temperature is less than 60°C
240 (Bijsterveld et al. 2001). Therefore, the testing temperature for binder high PG characterization in this
241 study was selected as 64°C, which is regarded as sufficient. The predetermined temperature was stabilized
242 within +/- 0.1°C tolerance for 10 minutes. The chosen two stress levels (0.1 kPa and 3.2 kPa) can
243 characterize both linear and non-linear responses of binders. The test protocol includes ten creep (1 s) -
244 recovery (9 s) cycles at each stress level. Before the twenty creep-recover cycles for the two stress levels,
245 a first ten cycles at 0.1 kPa were applied for conditioning the sample to reach the steady state to minimize

246 the effects of delayed elasticity (Golalipour 2011). The non-recoverable creep compliance (J_{nr}) and
247 percent recovery (R) were calculated. Since rutting is primarily critical during the earlier in-service period
248 of pavements at high temperatures, MSCR tests were performed on short-term aged binder samples to
249 simulate the aging after the road construction.

250 **4-mm DSR Test Method**

251 Using 4-mm parallel plates, FS tests from 1 to 100 rad/s were conducted at low temperatures from -30 to
252 10°C with an incremental step of 10°C. It was reported that DSR measurements at low temperatures may
253 generate errors in the values of dynamic data due to instrument compliance. Using small-diameter plates
254 with a high gap between the plates at low temperatures is recommended to reduce the instrument
255 compliance error (Schroter et al. 2006). In the current study, a gap of 3-mm between the plates was used
256 with the 4-mm parallel plate geometry, which was validated and recommended by other institutions
257 (Wang et al. 2019). Besides, automatic real-time compliance corrections were done using the pre-input
258 machine compliance for the 4-mm parallel plates on the measuring system. To accommodate the specimen
259 on such a small plate, a specifically designed butterfly silicone mold was manufactured to prepare and
260 install the samples on the DSR plates as shown in Figure 4. The detailed sample preparation steps can be
261 found in (Wang et al. 2019). When chamber temperature drops to -30°C, the resulting binder shrinkage
262 could potentially cause its de-bonding from the top plate. To ensure sufficient adhesion between the
263 sample and plates, the normal force was set automatically to zero during the cooling phase. For each type
264 of binder, a minimum of three replicates were tested and average results were reported.

265 **Frequency Sweep Test Method**

266 FS tests of CRMB and bitumen phase binder samples were conducted using the parallel-plate
267 configuration (25-mm diameter and 1-mm gap) from 0.1 to 100 rad/s at temperatures from 10 to 70°C. To
268 ensure measurements within the linear viscoelastic (LVE) range, a strain level of 0.1% under strain-
269 controlled mode was chosen.

270 Compared to binders, the viscoelastic response of swollen rubber is less sensitive to temperature.
271 Therefore, the rheological properties of swollen rubber were measured using the 8-mm parallel plates over
272 a temperature range of -10~130°C. The measurements were performed at a strain level of 1% under strain-
273 controlled mode from 0.1 to 100 rad/s. The detailed testing setup can be found in (Wang et al. 2020).

274 **RESULTS AND DISCUSSION**

275 **Repeatability of DSR Test Results**

276 For modified binders containing particulate matter such as crumb rubber, the variability of binder test
277 results is always a concern for accurate characterization. It was recommended that the gap between the
278 DSR parallel plates should be higher than four times the maximum particulate size (FHWA 2014). This is
279 to eliminate the influence of the particle-to-particle interaction between the parallel plates. Therefore,
280 considering the crumb rubber particle size in this study, the gap height might be accommodated to 2 mm.
281 However, to make comparable results with the conventional DSR setup of 25-mm diameter and 1-mm gap
282 for neat bitumen, the 1-mm gap setting was also applied to the tests of CRMB binders. Test results from
283 three replicates were compared as shown in Figure 5a to verify the validity of the 1-mm gap for CRMB
284 binders. It can be seen that the strain responses of three replicates at different creep-recovery cycles are
285 overlapped with each other. The calculated values of non-recoverable compliance and recovery at 3.2 kPa
286 are also shown in Figure 5a. The coefficients of variation for both $J_{nr,3.2}$, and $R_{3.2}$ are less than 10%, which
287 are generally acceptable for engineering purposes. In terms of the 4-mm DSR test, the variability of FS
288 test results is shown in Figure 5b. Both vertical and horizontal axes are plotted in the arithmetic scale to
289 more clearly see the variance of values. For both complex modulus and phase angle, the three replicates
290 yield quite close results.

291 To further check the result variability between different replicates, a one-way analysis of variance
292 (ANOVA) was performed on the measured values of complex modulus and phase angle. A confidence
293 level of 95% was used. The ANOVA results are summarized in Table 1. For either shear strain from
294 MSCR test or complex modulus and phase angle from 4-mm DSR FS test, the F value is smaller than the
295 F -critical, which means there is no significant difference between the results from the three replicates. In

296 addition, the *P-value* is much higher than the significance level, indicating the testing results are quite
297 repeatable and not affected by the rubber particle interactions or sample preparation process. Therefore,
298 the binder tests carried out in this study using the adopted DSR configurations have good repeatability.

299 **High-temperature Rutting Performance**

300 *Creep and Recovery Strain Response*

301 Figure 6 shows the strain responses of the first creep and recovery cycle at 3.2 kPa for different binders. A
302 semi-logarithmic plot was used to compare the strain difference more clearly. It can be found from Figure
303 6a that the accumulated strain of neat bitumen 70/100 increases dramatically under the creep stress. With
304 the increase of rubber content, less accumulated strains of CRMB binders were observed. For instance, the
305 accumulated strain of CRMB-22 after the creep stage was only around 12% of that of CRMB-5. The main
306 creep deformation of neat bitumen is viscous flow at high temperatures while for CRMB binders, it
307 changes to viscoelastic flow due to rubber modification. During the recovery stage, neat bitumen 70/100
308 almost shows no strain recovery, further indicating that viscous flow is the main type of creep deformation
309 for neat bitumen. It also implies that viscosity can be regarded as a primary parameter to characterize the
310 high-temperature performance of neat bitumen. By contrast, CRMB binders show obvious strain
311 recoveries due to the delayed elasticity. The higher the rubber content, the less non-recoverable strain
312 (permanent deformation). Viscosity is insufficient as a parameter to characterize the high-temperature
313 performance of CRMB binders. Therefore, parameters, which are capable of capturing the delayed
314 elasticity, should be developed to evaluate the rutting resistance of highly modified binders.

315 Figure 6b shows the effects of two warm-mix additives on the creeping and recovering properties of
316 binders. For the wax-based additive, it decreased the accumulated strain of neat bitumen during the creep
317 stage but did not significantly change the strain recovery ability. By contrast, the addition of wax-based
318 additives maintained the creep strain response but slightly increased the recoverable strain. In either way,
319 wax-additives can facilitate the deformation resistance of binders. For the chemical-based additive, it has
320 an insignificant effect on the creep-recovery response. However, it seemed to soften CRMB-22 by
321 increasing the accumulated creep strain and decreased the recoverable strain, hence reducing the

322 resistance to permanent deformation. Besides the above findings, the modification of warm-mix additives
323 did not change the main creep deformation mechanism of binders.

324 *Non-recoverable Compliance and Percentage Recovery*

325 Two parameters from MSCR test results, namely non-recoverable compliance and percentage recovery,
326 were used to capture the delayed elasticity and characterized the high-temperature properties of binders.
327 Table 2 summarizes MSCR test results of both neat bitumen and CRMB with warm-mix additives. It is
328 apparent that the J_{nr} values of bitumen at both stress levels significantly decreased as the rubber content
329 increased, indicating an improved rutting resistance of CRMB. In addition, CRMB binders had a
330 considerably higher ability to recover (R) than the unmodified bitumen 70/100 at both stress levels. The
331 lower J_{nr} and higher percent recovery of CRMB compared to neat bitumen resulted from the superior
332 polymer network established by the bitumen-rubber interaction (Wang et al. 2020).

333 With regard to warm-mix additives, the addition of wax-based additive to both 70/100 and CRMB-22
334 decreased the J_{nr} value but had an insignificant effect on the percent recovery. The increased resistance to
335 permanent deformation is attributed to the microcrystalline structure of the wax-based additive when
336 temperature drops below its melting temperature (around 110 °C). Uniformly distributed wax particles
337 will form lattice structures at service temperature (64 °C in this case) to stiffen the binder (Yu et al. 2016).
338 The chemical-based additive generally had insignificant effects on the MSCR results of neat bitumen. By
339 contrast, the chemical-based additive seemed to soften CRMB-22 and slightly decreased the percent
340 recovery.

341 The stress sensitivity parameter $J_{nr diff}$ seems to lack ubiquity to characterize the stress sensitivity of
342 CRMB binders. From Table 2, all CRMB binders except CRMB-5 and 70/100-W exceeded the maximum
343 allowable $J_{nr diff}$ value (75%) as stated in the specification AASHTO M 332-19. However, the low J_{nr}
344 values of these binders demonstrate that they have adequate resistance to permanent deformation. The
345 parameter $J_{nr diff}$ unfairly penalizes binders with low J_{nr} values. Alternatively, the most recent
346 specification AASHTO M 332-19 addresses the concern by removing the $J_{nr diff}$ requirement for binders

347 having a $J_{nr3.2}$ value of 0.5 kPa^{-1} or lower at the selected test temperature. To remedy the unsuitability of
 348 the $J_{nr diff}$ parameter for accreditation purposes, an alternate parameter $J_{nr slope}$ was proposed in Equation
 349 1. It is defined as the change in J_{nr} for an incremental change in applied stress τ (Stempihar et al. 2018).

$$J_{nr slope} = \frac{dJ_{nr}}{d\tau} = \frac{J_{nr3.2} - J_{nr0.1}}{\tau_{3.2} - \tau_{0.1}} \times 100 \quad (1)$$

350 Where $\tau_{3.2}$ and $\tau_{0.1}$ are the stress levels of 3.2 kPa and 0.1 kPa. $J_{nr3.2}$ and $J_{nr0.1}$ are the corresponding J_{nr}
 351 values at the two stress levels. From Table 2, it can be seen that all binders meet the requirement of stress
 352 sensitivity (lower than 75%) using the $J_{nr slope}$ parameter, which can be considered as a more appropriate
 353 representation of stress sensitivity. $J_{nr slope}$ was also reported to have a much better correlation with an
 354 incremental increase in rut depth (Stempihar et al. 2018). CRMB binders exhibited less stress sensitivity
 355 as expected using the new parameter. The acceptable $J_{nr3.2}$ and percent differences for varying levels of
 356 traffic are specified in AASHTO MP 19-10. Using the alternate parameter $J_{nr slope}$, the traffic level each
 357 binder can reach at the temperature of 64°C was also shown in Table 2. Neat bitumen with and without
 358 warm-mix additives are suitable for pavements with standard traffic conditions. With the increase of
 359 rubber content, CRMB can be used for heavier traffic conditions.

360 **Low-temperature Rheology and Performance Grading**

361 *Correlation between 4-mm DSR Measured Data and BBR Parameters*

362 While BBR is a flexural test in the time domain, DSR measures the shear rheological properties of binders
 363 in the time/frequency domain. Therefore, FS measurements from DSR must be mathematically
 364 transformed to be comparable to those from BBR. Previous studies have developed methods to convert
 365 DSR data into the parameters related to BBR tests (i.e., interconversion from dynamic frequency sweep to
 366 shear stress relaxation) as shown in Table 3. The corresponding low-temperature PG criteria for binders
 367 were also proposed using 4-mm DSR, and they are summarized in Table 3.

368 Regarding the methods of interconversion from dynamic FS to shear stress relaxation, both exact
 369 conversion methods based on linear viscoelastic theory and approximate conversion methods were used as

370 mentioned in Table 3. The exact interconversion using the generalized Maxwell model relates the shear
 371 relaxation modulus $G(t)$ in time domain to the storage modulus $G'(\omega)$ and loss modulus $G''(\omega)$ in the
 372 frequency domain by the following equations.

$$G(t) = \sum_{i=1}^n g_i e^{-t/\lambda_i} \quad (2)$$

$$G'(\omega) = \sum_{i=1}^n g_i \frac{\omega^2 \lambda_i^2}{1 + \omega^2 \lambda_i^2} \quad (3)$$

$$G''(\omega) = \sum_{i=1}^n g_i \frac{\omega \lambda_i}{1 + \omega^2 \lambda_i^2} \quad (4)$$

373 where g_i and λ_i define the discrete relaxation spectrum and represent the stiffness and relaxation time of
 374 the i^{th} Maxwell component. ω is the angular loading frequency from DSR tests. By fitting the dynamic
 375 frequency sweep data to Equations 3 and 4, the shear relaxation modulus in time domain can be obtained
 376 by Equation 2.

377 The shear stress relaxation modulus can also be converted from FS data by using the empirical conversion
 378 methods. The approximation method proposed by Ninomiya and Ferry (Ninomiya and Ferry 1959) is
 379 given in Equation 5.

$$G(t) = G'(\omega) - 0.4G''(0.4\omega) + 0.014G''(10\omega)|_{\omega=2/\pi t} \quad (5)$$

380 Alternatively, Christensen further simplified the approximate expression as

$$G(t) \approx G'(\omega)|_{\omega=2/\pi t} \quad (6)$$

381 After obtaining the relaxation modulus curve in the time domain, the m -value is determined as the
 382 relaxation rate at the time of interest. Lu *et al.* (Lu et al. 2017) utilized an approximate model originally
 383 proposed by Anderson *et al.* (Anderson et al. 1994) to correlate BBR creep stiffness with modulus from
 384 DSR. This model requires only the complex modulus and phase angle for the interconversion as shown in
 385 Equation 7. The m -value was also empirically approximated as Equation 8 at the temperature and
 386 frequency of interest.

$$S(t) = \frac{3G^*(\omega)}{1 + 0.2 \sin(2\delta)} \quad (7)$$

$$m = \delta/90 \quad (8)$$

387 Where $S(t)$ is creep stiffness at time t . δ is phase angle.

388 Similarly, Oshone (Oshone 2018) proposed empirical equations to determine creep stiffness and m -value
389 as shown in Equations 9 and 10.

$$S(t) = 1.28G^*(\omega) + 19.2 \quad (9)$$

$$m = 0.008\delta + 1 \quad (10)$$

390 Equations 7 and 9 are linear functions derived by empirically correlating DSR with BBR testing results.

391 Besides the interconversion process from the frequency domain to time domain, Hajj *et al.* (Hajj et al.
392 2019) also converted the shear response of binders to the uniaxial response using the following equation.

$$S(t) = G(t) (1 + 2\nu) \quad (11)$$

393 where ν is the Poisson's ratio of binder. It was assumed as 0.35 in this study, which was believed to be
394 more reasonable at low temperatures based on the laboratory test results (Benedetto et al. 2007). By doing
395 so, original grading criteria for BBR can be directly applied to the DSR derived parameters. It was
396 reported that the exact interconversion method (Equations 2-4) and approximate conversion method
397 (Equation 5) give an almost identical stress relaxation curve (Sui et al. 2011). For simplicity, the empirical
398 conversion method as shown in Equation 5 was used in this study.

399 *Black diagram*

400 The raw dynamic data of different binders from 4-mm DSR frequency sweep tests were compared in the
401 black diagrams (Figure 7). A black diagram is a useful tool to analyze the rheological data. It can identify
402 possible data discrepancies, verify time-temperature equivalence and thermo-rheological simplicity, and
403 compare different types of bitumen.

404 It can be seen from Figure 7 that there are no obvious discontinuities or sudden changes in the slope of the
405 curves. The smooth curves indicate that 4-mm DSR with the current test configurations can generate

406 reliable rheological data. The test samples are also confirmed as thermo-rheologically simple. Unlike the
 407 black diagrams in the high-temperature range (Wang et al. 2018), the curves of binders in the black space
 408 in the low-temperature range do not show any symbolic patterns. Although bitumen with the addition of
 409 CRM becomes more elastic as reflected by the shift of rheological data towards lower phase angle (left in
 410 the figure), the change in the elastic behavior is not as significant as in the high-temperature range. This is
 411 because, at low temperatures, the bitumen matrix is stiffer than rubber particles. From the
 412 micromechanical point of view, it has a more dominant impact than rubber particles on determining the
 413 rheological properties of CRMB. With the same phase angle value, CRMB binders exhibit lower complex
 414 moduli compared to unmodified bitumen. This implies that CRMB may possess improved low-
 415 temperature performance than unmodified bitumen, which will be discussed in the following subsections.

416 *Analysis methods for interpreting 4-mm DSR data*

417 There are two main transformations required to obtain BBR parameters from the DSR test results: (a)
 418 converting dynamic data from the frequency domain to the time domain, and (b) converting shear
 419 response to flexural response. Then, the critical cracking temperatures for low-temperature PG can be
 420 determined by the BBR criteria, i.e., $S(t)=300$ MPa and $m=0.30$ at $t=60$ s at PG temperature + 10°C. To
 421 demonstrate the calculation process, the neat bitumen 70/100 was taken as an example in this section.

- 422 • **Step 1.** The Christensen-Anderson-Marasteanu (CAM) model was used to build the viscoelastic
 423 master curves at a reference temperature using the FS data (Figure 8);
- 424 • **Step 2.** The shear stress relaxation modulus curve in time domain was converted using the
 425 approximation method as given in Equation 5. The master curves of storage modulus and loss
 426 modulus were derived by the following relationships.

$$G'(\omega) = |G^*| \sin \delta, \text{ and } G''(\omega) = |G^*| \cos \delta \quad (12)$$

- 427 • **Step 3.** Convert the shear relaxation modulus to flexural creep stiffness using Equation 11 as
 428 shown in Figure 9.

- 429 • **Step 4.** Determine the value of $S(t)$ and m -value at $t= 60$ s through the creep stiffness master
 430 curve. The m -value was determined by taking the first derivative after obtaining the trendline
 431 equation. The calculated values of S and m are shown in Table 4.
- 432 • **Step 5.** Calculate the critical cracking temperatures by interpolation. Steps 1-4 at a different
 433 reference temperature were repeated. The selected reference temperatures should bracket specified
 434 values of S and m . The critical cracking temperatures were thus determined by interpolating
 435 between passing and failing temperatures based on the limiting values of S and m (see Equations
 436 13 and 14).

$$T_{c,S} = T_1 + \frac{(T_1 - T_2)(\log 300 - \log S_1)}{\log S_1 - \log S_2} - 10 \quad (13)$$

$$T_{c,m} = T_1 + \frac{(T_1 - T_2)(0.3 - m_1)}{m_1 - m_2} - 10 \quad (14)$$

437 where $T_{c,S}$ and $T_{c,m}$ are the critical temperatures or true grade controlled by the creep stiffness and m -
 438 value respectively. T_1 is the temperature at which S or m passes the criterion while T_2 is the temperature at
 439 which S or m fails the criterion. S_1 and S_2 are the creep stiffness (MPa) at T_1 and T_2 . m_1 and m_2 are the
 440 creep rate at T_1 and T_2 .

441 *Critical cracking temperature and Delta T_c parameter*

442 Using the above calculation process, the derived values of S and m from 4-mm DSR test results at
 443 different temperatures are summarized in Table 4. In general, binders with a lower creep stiffness and a
 444 higher creep rate have improved resistance to thermal cracking. The values of S and m highlighted in bold
 445 and italic in Table 4 are the data that bracket the specifications and are used to calculate the critical
 446 cracking temperatures (Equations 13 and 14). It can be seen from Table 4 that there are no consistent
 447 trends for the change in creep stiffness and creep rate of different binders at different temperatures. At the
 448 temperatures that bracket the specifications (shaded data), the addition of wax-based additives to neat
 449 bitumen increased the creep stiffness and decreased the creep rate. This is because the wax may crystallize
 450 in binders at low temperatures, resulting in a stiffening effect. By contrast, the chemical-based additive

451 decreased the stiffness and increased the creep rate of the neat bitumen. The polymers and oils in the
 452 chemical additive may be conducive to improve the cracking resistance. Similar effects of warm-mix
 453 additive were found on CRMB. Briefly, wax-based additives negatively affect the thermal cracking
 454 performance of binders while chemical-based additives can improve the low-temperature performance.
 455 Comparing the neat bitumen with CRMB binders, rubber modification decreases the stiffness and
 456 increases the creep rate at low temperatures. Further increasing the rubber content, the improvement of
 457 low-temperature performance is more prominent. The above findings are consistent with previous BBR
 458 test results for characterizing the low-temperature performance of CRMB binders (Akisetty et al. 2010).

459 The low PGs of different binders based on the current PG specifications are also shown in Table 4. The
 460 addition of warm-mix additives does not change the low-temperature PG of neat bitumen as -28°C . The
 461 modification by CRM further decreases the low-temperature PG. When increasing the CRM content to
 462 22%, the low PG of CRMB is improved to -40°C compared to other CRMBs with lower CRM contents
 463 which have a low PG of -34°C . The wax-based additive increases the continuous low PG of CRMB by
 464 1.1°C while CRMB-22 with the chemical-based additive decreases the continuous low PG by 1.8°C .

465 Since the current PG grading system adopts an increment of 6°C , binders having the same PG may have a
 466 slightly different performance at a certain temperature. Therefore, the critical temperatures (true
 467 continuous grade) of different binders for low-temperature PG calculated using Equations 13 and 14 are
 468 summarized in Table 5. To account for the different governing mechanisms for the performance grade of a
 469 binder, a new parameter called ΔT_c was defined below

$$\Delta T_c = T_{c,s} - T_{c,m} \quad (15)$$

470 The sign of ΔT_c indicates whether the performance grade of the binder is governed by its creep stiffness
 471 ($+\Delta T_c$) or creep rate ($-\Delta T_c$). The absolute magnitude of ΔT_c indicates the degree to which the binder is
 472 governed by either creep stiffness or creep rate. ΔT_c values for different binders were shown in Table 5.

473 It can be seen from Table 5 that both $T_{c,S}$ and $T_{c,m}$ of CRMB gradually decrease as the increase of rubber
474 content, indicating a lower low-temperature PG. With regard to the effect of warm-mix additives, the
475 addition of wax-based additive increases the critical temperatures of both neat and rubber modified
476 binders while chemical-based additive slightly decreases the critical temperature. In addition, it is
477 noteworthy that the $T_{c,S}$ of 70/100 based binder (with/without warm additives) is higher than the
478 corresponding $T_{c,m}$, resulting in a positive value of ΔT_c . By contrast, CRMB based binder has the opposite
479 situation in which its $T_{c,S}$ is lower than $T_{c,m}$. However, there is not a clear trend of the effects of rubber
480 content and warm additives on the value of ΔT_c . The different signs of ΔT_c of neat bitumen and CRMB
481 implies that the low-temperature PG of 70/100 based binders are creep stiffness controlled while CRMB
482 binders are m -value controlled. Creep stiffness does not present a complete picture of binder cracking
483 tendency at low temperatures. This is because bitumen is a viscoelastic material, which is able to relax
484 applied stresses. In other words, if given sufficient time, bitumen will shed the built-up stresses when
485 applying a load or changing the temperature condition. This ability to relax the stresses of binders is
486 defined as creep rate or m -value in the BBR test.

487 Understanding the different controlling mechanisms can have two benefits in optimizing the binder design.
488 Firstly, neat bitumen is more suitable in the climates where rapid changes to cold temperatures are often
489 observed. This is because high m -value CRMB binders may encounter a rapid increase in thermal stress
490 that can lead to cracking before relaxation can occur (Marasteanu and Cannone Falchetto 2018). CRMB is
491 more suitable for climates where cold temperatures stay for an extended period because more relaxation of
492 CRMB takes place due to its higher m -value. Secondly, to further improve the low-temperature
493 performance grades of binders, different strategies should be used for neat bitumen and CRMB. For neat
494 bitumen, emphasis should be put on decreasing the creep stiffness while for CRMB, efforts should be
495 done in increasing the creep rate.

496 **Modification Mechanism for the High- and Low-temperature Performance**

497 CRMB can be regarded as a binary composite in which rubber particles are embedded in the bitumen
498 matrix. To figure out how the rubber modification and warm-mix additives influence the binder
499 performance, the bitumen and rubber phases of CRMB-22, CRMB-22-W and CRMB-22-C were separated,
500 and their rheological properties were investigated through frequency sweep tests. In general, bitumen-
501 rubber interaction controls the binder properties through the following ways: (1) changing the mechanical
502 properties of bitumen matrix due to the loss of light fractions absorbed by rubber and the potential
503 released components from rubber; (2) changing the mechanical properties of rubber due to rubber
504 swelling; (3) changing the volume fraction of rubber due to swelling (Wang et al. 2020). With the
505 obtained viscoelastic data at various frequencies and temperatures, master curves were established based
506 on the time-temperature superposition principle (TTSP).

507 *Effect of Rubber Modification*

508 Figure 10 presents the viscoelastic master curves of bitumen and rubber phases at a reference temperature
509 of 30°C. Firstly, comparing neat bitumen 70/100 and CRMB-22, CRMB-22 has higher complex moduli
510 than 70/100 at low frequencies (high temperatures) and lower complex modulus at high frequencies (low
511 temperatures). In the whole frequency range, the phase angle of CRMB-22 is lower than that of 70/100,
512 indicating more elastic behaviors. Considering low/high frequencies correspond to high/low temperatures
513 in the frame of master curves, CRMB-22 is stiffer than 70/100 at high temperatures while softer at low
514 temperatures. This coincides with the finding that CRMB-22 has improved both high-temperature rutting
515 and low-temperature cracking performance. Secondly, it can be found that the bitumen phase CRMB-22-
516 BP is stiffer and more elastic than neat bitumen 70/100 because of the loss of light components absorbed
517 by rubber particles, which increases the proportions of asphaltenes in bitumen. Asphaltenes are primarily
518 responsible for the increase of complex modulus and decrease of phase angles (Apostolidis et al. 2017).
519 Thirdly, comparing the bitumen phase (CRMB-22-BP) with the swollen rubber phase, the swollen rubber
520 sample has lower moduli at high frequencies and higher moduli at low frequencies. This means CRMB-22
521 will have a smaller creep stiffness and a higher creep rate than the neat bitumen at low temperatures,

522 which is exactly the same as measured in the 4-mm DSR tests. Standing from a micromechanics point of
523 view, the property changes of the bitumen phase and the inclusion of swollen rubber particles in the
524 bitumen matrix together contribute to the peculiar viscoelastic response of CRMB-22, i.e., stiffer and
525 more elastic at high temperatures, softer and more elastic at low temperatures. This finding was also
526 verified by the authors using micromechanical modelling (Wang et al. 2020). These peculiar viscoelastic
527 responses of CRMB-22 explain why CRMB in general has improved resistance to both rutting and
528 thermal cracking.

529 *Effect of Warm-mix Additives*

530 The warm additives were added to CRMB binders at a relatively low temperature after the bitumen-rubber
531 mixing process. Therefore, the additives mainly influence the properties of the bitumen matrix instead of
532 the rubber phase (Yu et al. 2017). Figure 11 presents the viscoelastic master curves of bitumen phases
533 containing warm-mix additives at a 30°C. For neat bitumen 70/100, the addition of wax-based additives
534 resulted in a significant increase in complex modulus and reduction in phase angle. The reason has been
535 explained before, which is due to the stiffening effect of wax. By contrast, the addition of chemical-based
536 additives seemed to slightly soften the binder. Chemical-based additives had insignificant effects on the
537 viscoelastic properties of binders. Comparing the bitumen phases of CRMB binders with and without
538 additives, similar effects of warm additives on the properties of bitumen phases were observed. The
539 findings from the viscoelastic master curves further verify the conclusions in the previous sections and
540 reveal how additives influence the high- and low-temperature performance of binders. Based on the above
541 analysis, it should be noted that although warm-mix additives can be used to effectively reduce the
542 viscosity of CRMB and hence reduce the construction temperatures, the type of additives should be
543 cautiously selected to ensure the high- and low-temperature performance are not compromised.

544 **CONCLUSIONS AND RECOMMENDATIONS**

545 The present study investigated the high- and low-temperature performance of warm crumb rubber
546 modified bitumen (CRMB) binders using MSCR and low-temperature FS tests. The obtained relaxation
547 parameters from 4-mm DSR tests were used to determine the low-temperature PG by directly applying the

548 BBR criterion. Two transformations were done in this process, namely converting viscoelastic master
549 curves from the frequency domain to the shear relaxation modulus in the time domain, and converting
550 shear response to flexural response by assuming a constant Poisson's ratio. The rheology of the bitumen
551 and rubber phases of CRMB was investigated to gain insights into the rubber and additives modification
552 mechanism and its impact on the binder performance. The following conclusions can be drawn:

- 553 • CRMB binders have superior rutting and thermal cracking resistance due to rubber modification.
554 The improvement of high- or low-temperature performance is more prominent at higher rubber
555 concentrations.
- 556 • Warm-mix additives have different effects on high- or low-temperature performance. Generally,
557 the wax-based additive improves the rutting resistance while having adverse effects on the low-
558 temperature performance. By contrast, chemical-based additive slightly impairs the high-
559 temperature rutting resistance while improving the low-temperature performance.
- 560 • In terms of the critical cracking temperature, the low-temperature PG of 70/100 based binders is
561 creep stiffness controlled while CRMB binders are *m*-value controlled. Rubber modification
562 changes the controlling mechanism of low-temperature performance.
- 563 • The stiffening of the bitumen phase and the inclusion of swollen rubber particles in the bitumen
564 matrix together contribute to the peculiar viscoelastic response of CRMB, i.e., stiffer and more
565 elastic at high temperatures, softer and more elastic at low temperatures. This modification
566 mechanism explains the superior rutting and thermal cracking resistance of CRMB.
- 567 • Although warm-mix additives can effectively reduce the viscosity of CRMB and hence reduce the
568 construction temperatures, the type of additives should be cautiously chosen to ensure high- and
569 low-temperature performance are not compromised.

570 In future studies, BBR tests on binders can be performed to further verify the conclusions from 4-mm
571 DSR tests. High- and low-temperature performance of asphalt mastic and mixture are recommended to be
572 investigated to verify the findings at the binder level.

573 **DATA AVAILABILITY STATEMENT**

574 All data, models, and code generated or used during the study appear in the submitted article.

575

576 **REFERENCES**

- 577 Akisetty, C. K., Lee, S.-J., and Amirkhanian, S. N. (2009). "High temperature properties of rubberized
578 binders containing warm asphalt additives." *Construction and Building Materials*, 23(1), 565-573.
- 579 Akisetty, C. K., Lee, S. J., and Amirkhanian, S. N. (2010). "Laboratory investigation of the influence of
580 warm asphalt additives on long-term performance properties of CRM binders." *Int J Pavement*
581 *Eng*, 11(2), 153-160.
- 582 Anderson, D. A., Christensen, D. W., Bahia, H. U., Dongre, R., Sharma, M. G., and Antle, C. E. (1994).
583 "Binder Characterization and Evaluation Volume 3: Physical Characterization." *Strategic*
584 *Highway Research Program A-369* Washington, D.C., US.
- 585 Anderson, D. A., and Kennedy, T. W. (1993). "Development of SHRP binder specification." *Journal of the*
586 *Association of Asphalt Paving Technologists*, 62, 481-507.
- 587 Apostolidis, P., Liu, X., Kasbergen, C., and Scarpas, A. T. (2017). "Synthesis of Asphalt Binder Aging and
588 the State of the Art of Antiaging Technologies." *Transportation Research Record: Journal of the*
589 *Transportation Research Board*, 2633, 147-153.
- 590 Bahia, H. U., Hanson, D. I., Zeng, M., Zhai, H., Khatri, M. A., and Anderson, R. M. (2001).
591 "Characterization of Modified Asphalt Binders in Superpave Mix Design." *NCHRP Report 459*,
592 Transportation Research Board, Washington D.C.
- 593 Bahia, H. U., Zhai, H., and Range, A. (1998). "Evaluation of Stability, Nature of Modifier, and Short-Term
594 Aging of Modified Binders Using New Tests: LAST, PAT, and Modified RTFO." *Transp Res*
595 *Record*.
- 596 Bahia, H. U., Zhai, H., Zeng, M., Hu, Y., and Turner, P. (2001). "Development of Binder Specification
597 Parameters Based on Characterization of Damage Behavior." *Journal of the Association of*
598 *Asphalt Paving Technologists*, 70, 442-470.
- 599 Benedetto, H. D., Delaporte, B., and Sauzéat, C. (2007). "Three-Dimensional Linear Behavior of
600 Bituminous Materials: Experiments and Modeling." *Int J Geomech*, 7(2), 149-157.
- 601 Bijsterveld, W. T. v., Houben, L. J. M., Scarpas, A., and Molenaar, A. A. A. (2001). "Using Pavement as
602 Solar Collector: Effect on Pavement Temperature and Structural Response." *Transportation*
603 *Research Record: Journal of the Transportation Research Board*, 1778(1), 140-148.
- 604 D'Angelo, J., Kluttz, R., Dongre, R. N., Stephens, K., and Zanzotto, L. (2007). "Revision of the Superpave
605 High Temperature Binder Specification: The Multiple Stress Creep Recovery Test." *Journal of the*
606 *Association of Asphalt Paving Technologists*, 76, 123-162.
- 607 D'Angelo, J. A. (2009). "The Relationship of the MSCR Test to Rutting." *Road Materials and Pavement*
608 *Design*, 10(sup1), 61-80.
- 609 Daly, W., and Negulescu, I. (1997). "Characterization of asphalt cements modified with crumb rubber
610 from discarded tires." *Transportation Research Record: Journal of the Transportation Research*
611 *Board*(1583), 37-44.
- 612 De Visscher, J., and Vanelstraete, A. (2004). "Practical test methods for measuring the zero shear viscosity
613 of bituminous binders." *Materials and Structures*, 37(5), 360-364.
- 614 Farrar, M., Sui, C., Salmans, S., and Qin, Q. (2015). "Determining the Low-Temperature Rheological
615 Properties of Asphalt Binder Using a Dynamic Shear Rheometer (DSR)." *Fundamental Properties*
616 *of Asphalts and Modified Asphalts III Product: FP 08*, Western Research Institute, Laramie, WY
617 82072.
- 618 Farrar, M. J., Hajj, E. Y., Planche, J.-P., and Alavi, M. Z. (2013). "A method to estimate the thermal stress
619 build-up in an asphalt mixture from a single-cooling event." *Road Materials and Pavement*

- 620 *Design*, 14(sup1), 201-211.
- 621 Farshidi, F., Jones, D., and Harvey, J. T. (2013). "Warm-Mix Asphalt Study: Evaluation of Rubberized
622 Hot- and Warm-Mix Asphalt with Respect to Emissions." *Research Report: UCPRC-RR-2013-03*,
623 University of California Pavement Research Center, Davis, California, USA.
- 624 FHWA (2014). "Use of Recycled Tire Rubber to Modify Asphalt Binder and Mixtures." Federal Highway
625 Administration.
- 626 Golalipour, A. (2011). "Modification of Multiple Stress Creep and Recovery Test Procedure and Usage in
627 Specification."
- 628 Hajj, R., and Bhasin, A. (2017). "The search for a measure of fatigue cracking in asphalt binders – a
629 review of different approaches." *Int J Pavement Eng*, 19(3), 205-219.
- 630 Hajj, R., Filonzi, A., Rahman, S., and Bhasin, A. (2019). "Considerations for using the 4 mm Plate
631 Geometry in the Dynamic Shear Rheometer for Low Temperature Evaluation of Asphalt Binders."
632 *Transp Res Record*, 2673(11), 649-659.
- 633 Isacson, U., and Lu, X. (1995). "Testing and Appraisal of Polymer-Modified Road Bitumens - State-of-
634 the-Art." *Materials and Structures*, 28(177), 139-159.
- 635 Kim, H., Jeong, K.-D., Lee, M. S., and Lee, S.-J. (2014). "Performance properties of CRM binders with
636 wax warm additives." *Construction and Building Materials*, 66, 356-360.
- 637 Kim, H. S., Lee, S. J., and Amirhanian, S. (2010). "Rheology investigation of crumb rubber modified
638 asphalt binders." *Ksce J Civ Eng*, 14(6), 839-843.
- 639 Leng, Z., Padhan, R. K., and Sreeram, A. (2018). "Production of a sustainable paving material through
640 chemical recycling of waste PET into crumb rubber modified asphalt." *Journal of Cleaner
641 Production*, 180, 682-688.
- 642 Leng, Z., Yu, H., Zhang, Z., and Tan, Z. (2017). "Optimizing the mixing procedure of warm asphalt rubber
643 with wax-based additives through mechanism investigation and performance characterization."
644 *Construction and Building Materials*, 144, 291-299.
- 645 Lu, X., Uhlback, P., and Soenen, H. (2017). "Investigation of bitumen low temperature properties using a
646 dynamic shear rheometer with 4mm parallel plates." *International Journal of Pavement Research
647 and Technology*, 10(1), 15-22.
- 648 Marasteanu, M. O., and Cannone Falchetto, A. (2018). "Review of experimental characterisation and
649 modelling of asphalt binders at low temperature." *Int J Pavement Eng*, 19(3), 279-291.
- 650 Morea, F., Agnusdei, J. O., and Zerbino, R. (2010). "The use of asphalt low shear viscosity to predict
651 permanent deformation performance of asphalt concrete." *Materials and Structures*, 44(7), 1241-
652 1248.
- 653 Nanjegowda, V. H., and Biligiri, K. P. (2020). "Recyclability of rubber in asphalt roadway systems: A
654 review of applied research and advancement in technology." *Resources, Conservation and
655 Recycling*, 155.
- 656 Ninomiya, K., and Ferry, J. D. (1959). "Some approximate equations useful in the phenomenological
657 treatment of linear viscoelastic data." *Journal of Colloid Science*, 14(1), 36-48.
- 658 Oshone, M. T. (2018). "Performance based evaluation of cracking in asphalt concrete using viscoelastic
659 and fracture properties." Doctor of Philosophy, University of New Hampshire, New Hampshire,
660 US.
- 661 Schroter, K., Hutcheson, S. A., Shi, X., Mandanici, A., and McKenna, G. B. (2006). "Dynamic shear
662 modulus of glycerol: corrections due to instrument compliance." *J Chem Phys*, 125(21), 214507.
- 663 Sebaaly, P. E., Gopal, V. T., and Epps, J. A. (2003). "Low Temperature Properties of Crumb Rubber
664 Modified Binders." *Road Materials and Pavement Design*, 4(1), 29-49.
- 665 Singh, D., Sawant, D., and Xiao, F. (2017). "High and intermediate temperature performance evaluation of
666 crumb rubber modified binders with RAP." *Transportation Geotechnics*, 10, 13-21.
- 667 State of California Department of Transportation (2003). "Asphalt Rubber Usage Guide." State of
668 California Department of Transportation, Sacramento, CA, USA.
- 669 Stempihar, J., Gundla, A., and Underwood, B. S. (2018). "Interpreting Stress Sensitivity in the Multiple
670 Stress Creep and Recovery Test." *J Mater Civil Eng*, 30(2).

- 671 Sui, C., Farrar, M., Harnsberger, P., Tuminello, W., and Turner, T. (2011). "New Low-Temperature
672 Performance-Grading Method." *Transportation Research Record: Journal of the Transportation
673 Research Board*, 2207, 43-48.
- 674 Sui, C., Farrar, M., Tuminello, W., and Turner, T. (2010). "New Technique for Measuring Low-
675 Temperature Properties of Asphalt Binders with Small Amounts of Material." *Transportation
676 Research Record: Journal of the Transportation Research Board*, 2179, 23-28.
- 677 Sybilski, D. (1994). "Relationship between Absolute Viscosity of Polymer-Modified Bitumens and
678 Rutting Resistance of Pavement." *Materials and Structures*, 27(166), 110-120.
- 679 Wang, D., Cannone Falchetto, A., Alisov, A., Schrader, J., Riccardi, C., and Wistuba, M. P. (2019). "An
680 Alternative Experimental Method for Measuring the Low Temperature Rheological Properties of
681 Asphalt Binder by Using 4mm Parallel Plates on Dynamic Shear Rheometer." *Transportation
682 Research Record: Journal of the Transportation Research Board*, 2673(3), 427-438.
- 683 Wang, H., Apostolidis, P., Zhu, J., Liu, X., Skarpas, A., and Erkens, S. (2020). "The role of
684 thermodynamics and kinetics in rubber-bitumen systems: a theoretical overview." *Int J Pavement
685 Eng*, 1-16.
- 686 Wang, H., Liu, X., Apostolidis, P., Erkens, S., and Skarpas, A. (2020). "Experimental Investigation of
687 Rubber Swelling in Bitumen." *Transportation Research Record: Journal of the Transportation
688 Research Board*, 2674(2), 203-212.
- 689 Wang, H., Liu, X., Apostolidis, P., and Scarpas, T. (2018). "Non-Newtonian Behaviors of Crumb Rubber-
690 Modified Bituminous Binders." *Applied Sciences*, 8(10), 1760.
- 691 Wang, H., Liu, X., Apostolidis, P., and Scarpas, T. (2018). "Review of warm mix rubberized asphalt
692 concrete: Towards a sustainable paving technology." *Journal of Cleaner Production*, 177, 302-
693 314.
- 694 Wang, H., Liu, X., Apostolidis, P., and Scarpas, T. (2018). "Rheological Behavior and Its Chemical
695 Interpretation of Crumb Rubber Modified Asphalt Containing Warm-Mix Additives." *696 Transportation Research Record: Journal of the Transportation Research Board*, 2672(28), 337-
697 348.
- 698 Wang, H., Liu, X., Apostolidis, P., van de Ven, M., Erkens, S., and Skarpas, A. (2020). "Effect of
699 laboratory aging on chemistry and rheology of crumb rubber modified bitumen." *Materials and
700 Structures*, 53(2).
- 701 Wang, H., Liu, X., van de Ven, M., Lu, G., Erkens, S., and Skarpas, A. (2020). "Fatigue performance of
702 long-term aged crumb rubber modified bitumen containing warm-mix additives." *Construction
703 and Building Materials*, 239.
- 704 Wang, H., Liu, X., Zhang, H., Apostolidis, P., Erkens, S., and Skarpas, A. (2020). "Micromechanical
705 modelling of complex shear modulus of crumb rubber modified bitumen." *Materials & Design*,
706 188.
- 707 Wang, H., Liu, X., Zhang, H., Apostolidis, P., Scarpas, T., and Erkens, S. (2020). "Asphalt-rubber
708 interaction and performance evaluation of rubberised asphalt binders containing non-foaming
709 warm-mix additives." *Road Materials and Pavement Design*, 21(6), 1612-1633.
- 710 Wang, T., Xiao, F., Amirkhanian, S., Huang, W., and Zheng, M. (2017). "A review on low temperature
711 performances of rubberized asphalt materials." *Construction and Building Materials*, 145, 483-
712 505.
- 713 Yu, H., Leng, Z., Dong, Z., Tan, Z., Guo, F., and Yan, J. (2018). "Workability and mechanical property
714 characterization of asphalt rubber mixtures modified with various warm mix asphalt additives." *715 Construction and Building Materials*, 175, 392-401.
- 716 Yu, H., Leng, Z., and Gao, Z. (2016). "Thermal analysis on the component interaction of asphalt binders
717 modified with crumb rubber and warm mix additives." *Construction and Building Materials*, 125,
718 168-174.
- 719 Yu, H., Leng, Z., Xiao, F., and Gao, Z. (2016). "Rheological and chemical characteristics of rubberized
720 binders with non-foaming warm mix additives." *Construction and Building Materials*, 111, 671-
721 678.

- 722 Yu, H., Leng, Z., Zhou, Z., Shih, K., Xiao, F., and Gao, Z. (2017). "Optimization of preparation procedure
723 of liquid warm mix additive modified asphalt rubber." *Journal of Cleaner Production*, 141, 336-
724 345.
- 725 Zhang, J. P., Yang, F. H., Pei, J. Z., Xu, S. C., and An, F. W. (2015). "Viscosity-temperature characteristics
726 of warm mix asphalt binder with Sasobit (R)." *Construction and Building Materials*, 78, 34-39.
727

728 **Table 1.** One-way ANOVA results between different replicates of CRMB-22.

Source of variation		SS	DF	MS	F	P-value	F-critical
MSCR	Shear strain	40993.33	2	20496.67	0.3387	0.7127	2.9972
4-mm DSR FS	Complex modulus	6.82E+09	2	3.41E+09	0.2667	0.7669	3.1588
	Phase angle	0.0197	2	0.0098	0.0021	0.9979	3.1682

729 *Note: SS=Sum of Squares, DF=degree of freedom, MS= Mean Square.

730

731 **Table 2.** Summary of MSCR results of different binders at the short-term aged state.

Binder type	J_{nr} (1/kPa)		$J_{nr\text{diff}}$ (%)	$J_{nr\text{slope}}$ (%)	R (%)		Traffic level*
	0.1 kPa	3.2 kPa			0.1 kPa	3.2 kPa	
70/100	3.489	3.938	12.87	14.48	1.55	0.00	S
70/100-W	0.602	2.478	311.63	60.52	45.78	0.18	S
70/100-C	3.323	3.778	13.69	14.68	1.52	0.00	S
CRMB-5	1.336	1.780	33.23	14.33	22.35	3.73	H
CRMB-10	0.466	0.914	96.14	14.45	48.12	15.47	V
CRMB-15	0.142	0.413	192.86	8.71	76.32	32.45	E
CRMB-22	0.022	0.182	727.27	5.16	91.44	41.66	E
CRMB-22-W	0.019	0.176	826.32	5.06	93.42	45.69	E
CRMB-22-C	0.046	0.292	534.78	7.94	86.57	35.26	E

732 *Note: S=Standard, H=Heavy, V=Very Heavy, E=Extremely Heavy.

733

734 **Table 3.** Methods and criteria for low-temperature grading binders using 4-mm DSR.

Reference	Conversion methods	Creep stiffness grading criterion	m -value grading criterion
Sui et al. 2011	Generalized Maxwell model or Ninomiya and Ferry approximation method	$G(t) < 180$ MPa at $t=7200$ s at actual PG temperature	$m > 0.26$ from $G(t)$ at $t=7200$ s at actual PG temperature
Farrar et al. 2015	Christensen approximation method	$G(t) < 143$ MPa at $t=60$ s at PG temperature + 10°C	$m > 0.28$ from $G(t)$ at $t=60$ s at PG temperature + 10°C
Lu et al. 2017	Empirical Equation 7	$S(t) < 143$ MPa at $t=60$ s at PG temperature + 10°C	$m > 0.28$ at $\omega = 2/\pi t$ at PG temperature + 10°C
Oshone 2018	Empirical Equation 9	NA	NA
Hajj et al. 2019	Ninomiya and Ferry approximation method	$S(t) < 300$ MPa at $t=60$ s at PG temperature + 10°C	$m > 0.30$ from $S(t)$ at $t=60$ s at PG temperature + 10°C

735

736 **Table 4.** Creep stiffness and m -value derived from 4-mm DSR test results.

Binder type	-18°C		-24°C		-30°C		-36°C		Continuous low PG (°C)	Low PG (°C)
	S (MPa)	m	S (MPa)	m	S (MPa)	m	S (MPa)	m		
70/100	174.7	0.35	402.4	0.28	785.2	0.20	1112.4	0.16	-31.9	-28
70/100-W	216.1	0.33	625.9	0.24	1283.8	0.15	1453.9	0.13	-29.9	-28
70/100-C	161.7	0.37	466.0	0.28	1092.8	0.17	1394.4	0.13	-31.5	-28
CRMB-5	107.1	0.38	253.2	0.31	524.7	0.24	797.2	0.19	-34.7	-34
CRMB-10	92.0	0.39	223.9	0.32	469.6	0.25	723.8	0.20	-35.7	-34
CRMB-15	70.9	0.40	163.2	0.33	333.6	0.27	595.7	0.21	-37.1	-34
CRMB-22	56.0	0.42	124.9	0.36	252.3	0.30	453.9	0.24	-40.4	-40
CRMB-22-W	66.1	0.42	156.9	0.35	277.4	0.29	459.2	0.23	-39.3	-34
CRMB-22-C	61.2	0.43	134.1	0.37	237.7	0.31	443.9	0.26	-42.2	-40

737

738

739 **Table 5.** Critical cracking temperatures and ΔT_c values for different binders.

Binder type	70/100	70/100-W	70/100-C	CRMB-5	CRMB-10	CRMB-15	CRMB-22	CRMB-22-W	CRMB-22-C
$T_{c,S}$	-31.9	-29.8	-31.5	-35.4	-36.4	-39.1	-41.8	-40.9	-42.2
$T_{c,m}$	-32.2	-30.1	-32.5	-34.7	-35.7	-37.1	-40.4	-39.3	-41.1
ΔT_c	0.3	0.3	1.0	-0.7	-0.7	-2.0	-1.4	-1.6	-1.1

740

741

742

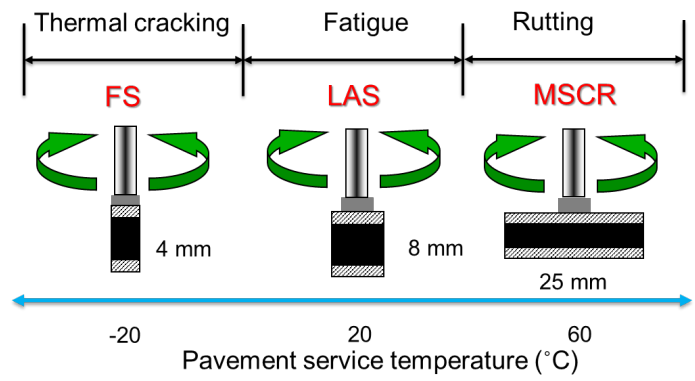
743

744

745

1

2



3

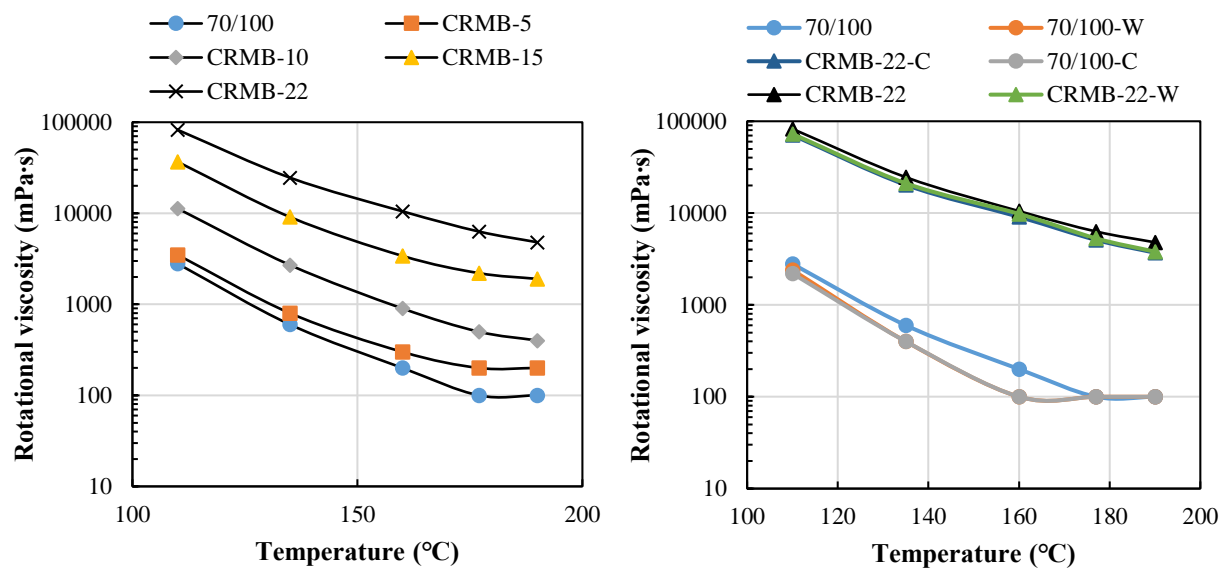
4

Figure 1. Unified DSR method for binder performance characterization from low to high temperatures.

5

1

2

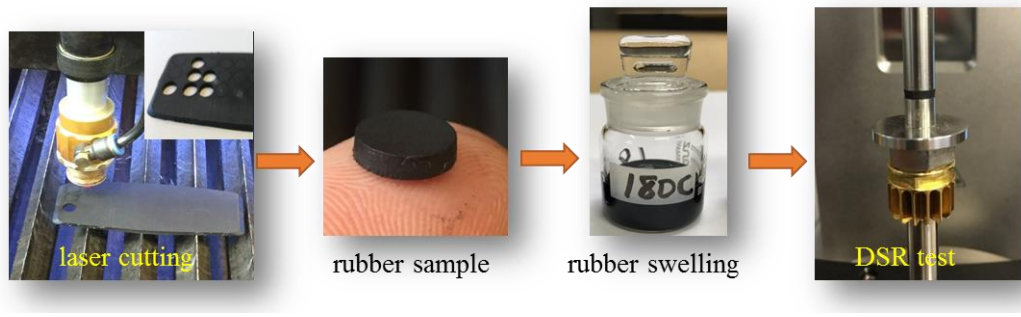


3

4

5 **Figure 2.** Rotational viscosities of CRMB binders with (a) different rubber contents; (b) warm-mix
6 additives.

7

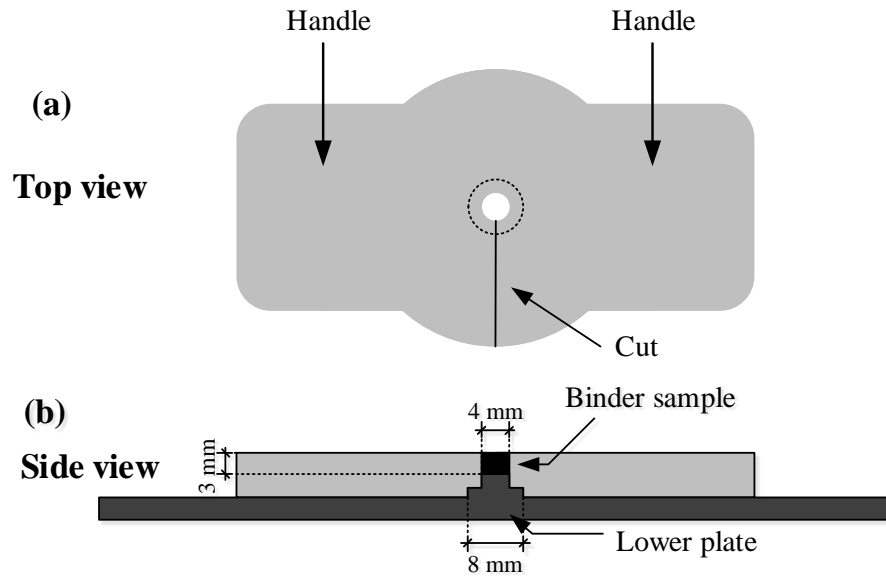


1

2

3

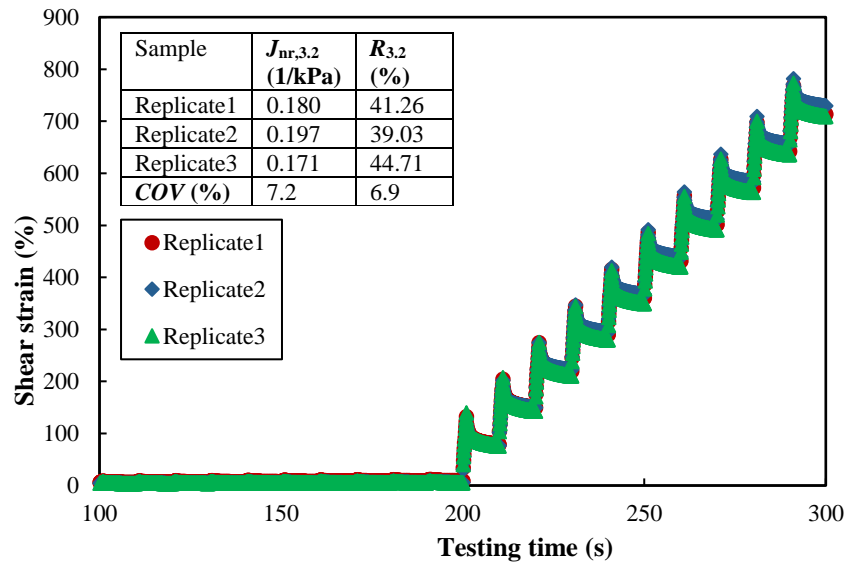
Figure 3. Dry and swollen rubber samples for DSR tests.



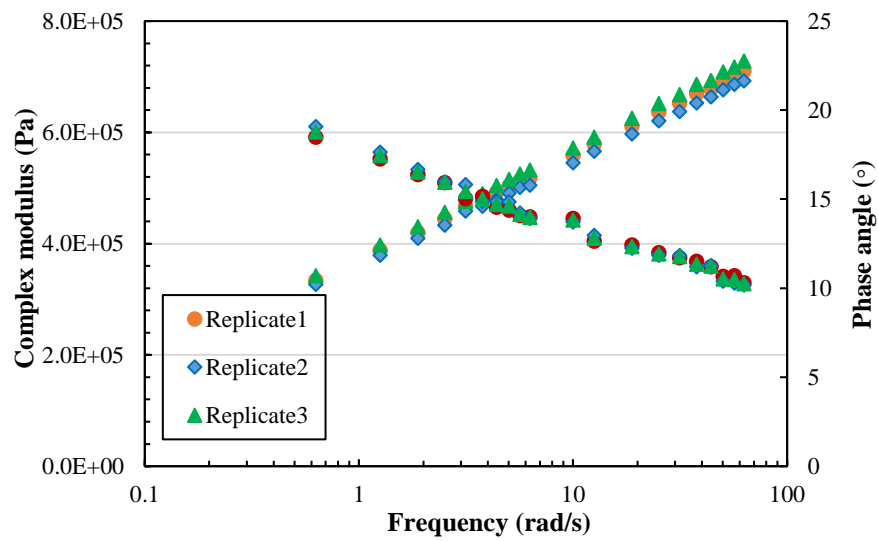
1

2 **Figure 4.** The butterfly silicone mold for 4-mm DSR sample installation: (a) top view; (b) side view.

3



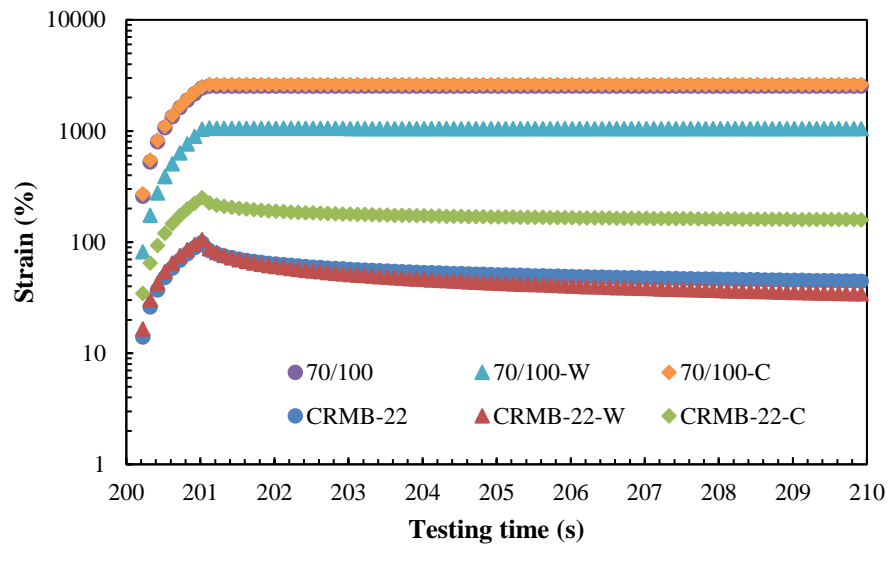
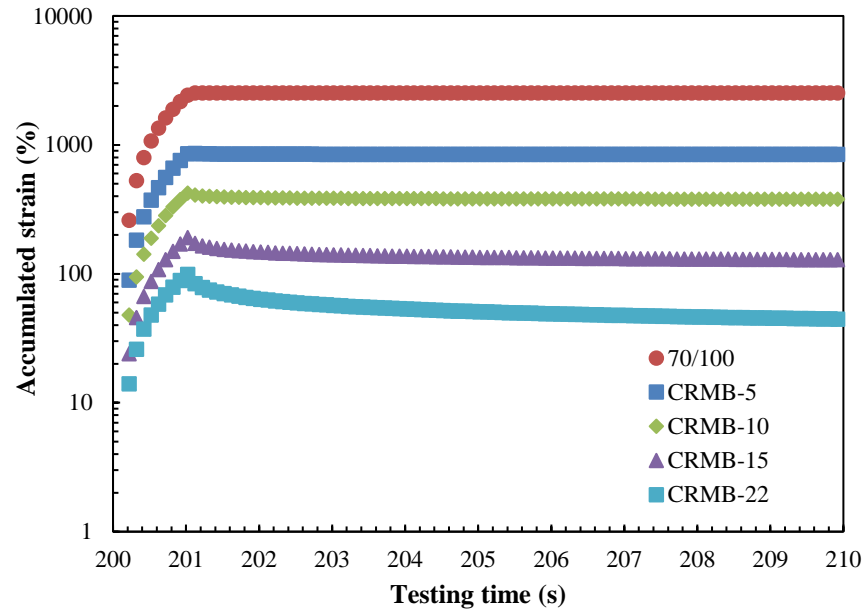
(a)



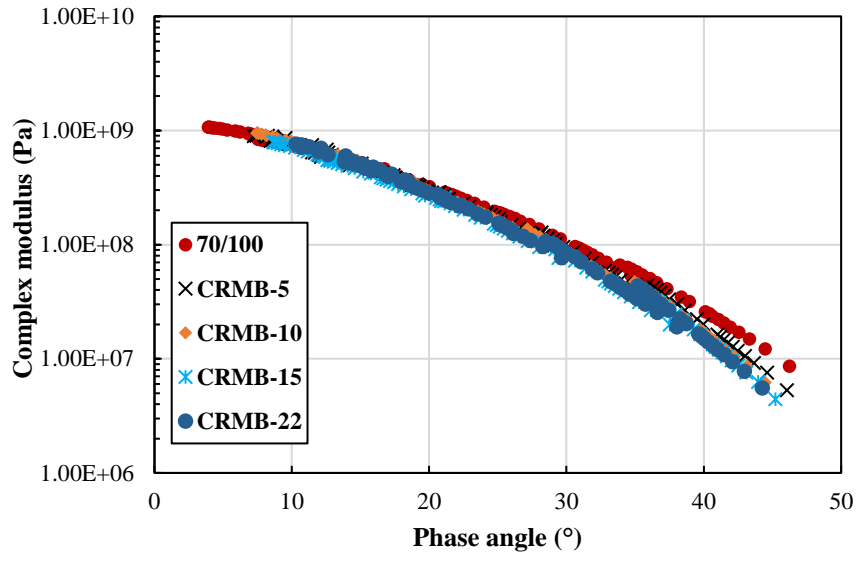
(b)

3 **Figure 5.** Variability of binder test results from CRMB-22 samples: (a) MSCR test using 25-mm plates at
 4 64 °C; (b) Frequency sweep test using 4-mm plates at -30 °C. (COV=coefficient of variation)

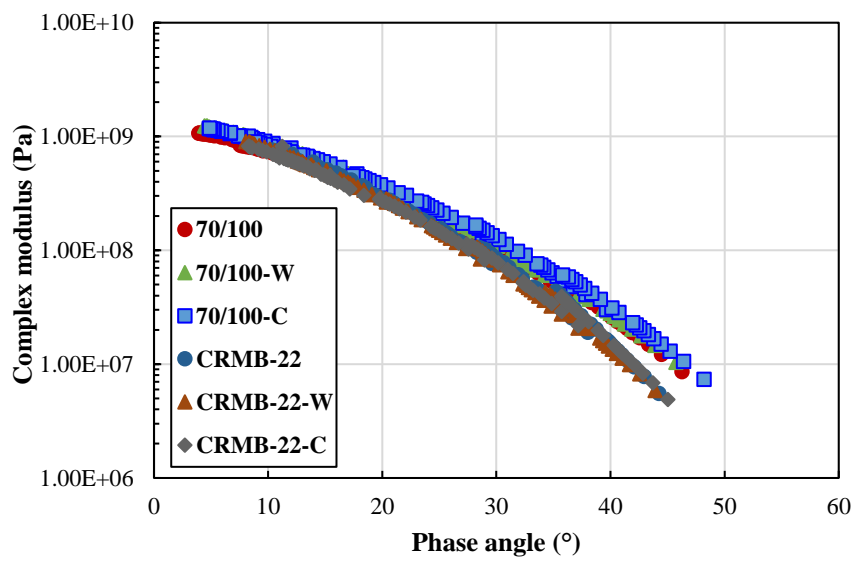
5



3 **Figure 6.** Creep and recovery strain responses of different binders at 3.2 kPa: (a) CRMB with different
 4 rubber contents; (b) Binders with warm-mix additives.

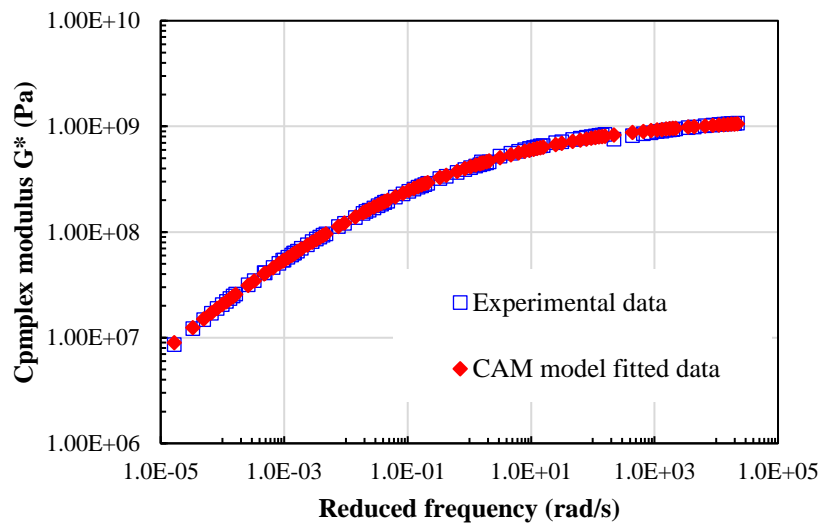


(a)



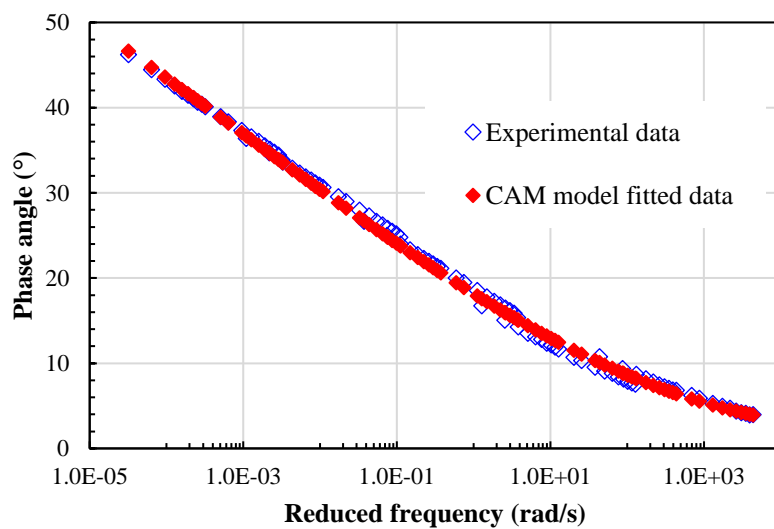
(b)

3 **Figure 7.** Black diagram of (a) CRMB binders and (b) binders with warm-mix additives.



1

(a)

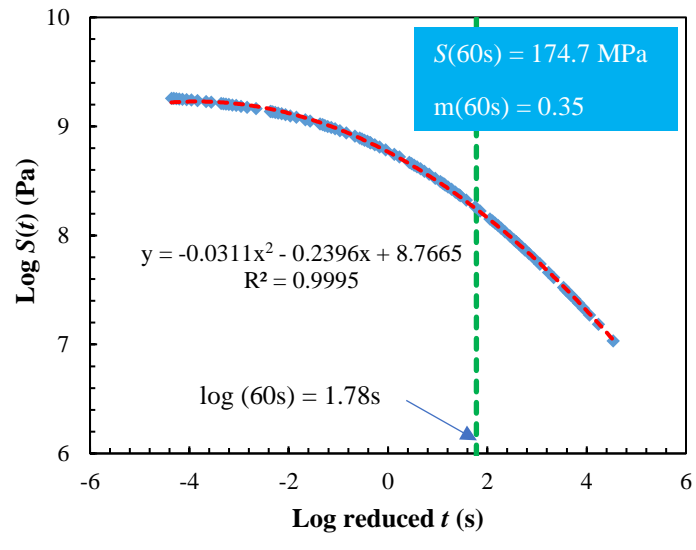


2

(b)

3 **Figure 8.** (a) Complex modulus and (b) phase angle master curves of neat bitumen 70/100 at a reference
4 temperature of -18°C .

5



1

2 **Figure 9.** Master curve of creep stiffness at a reference temperature of -18 °C.

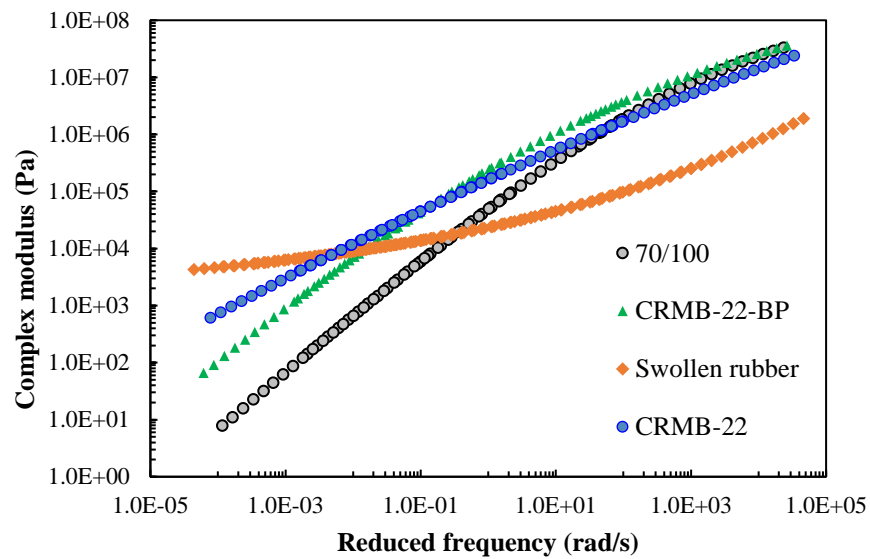
3

4

5

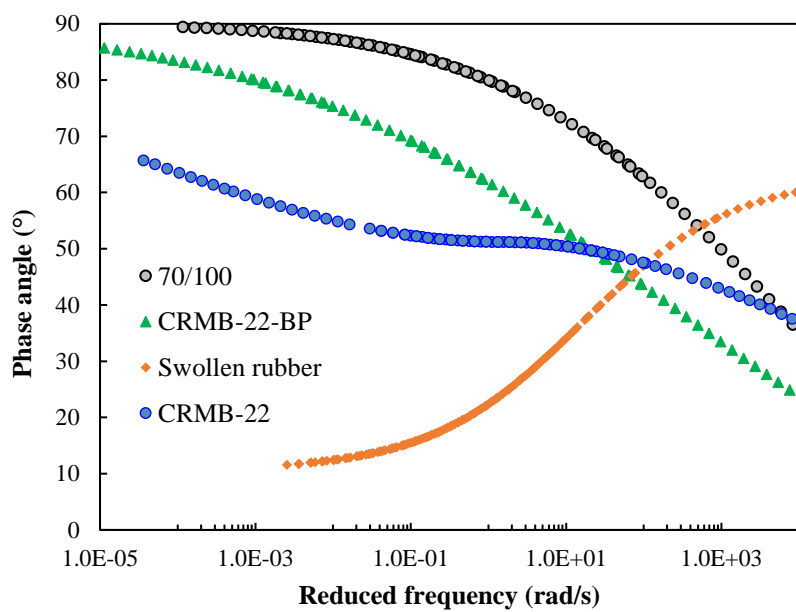
6

7



1

(a)

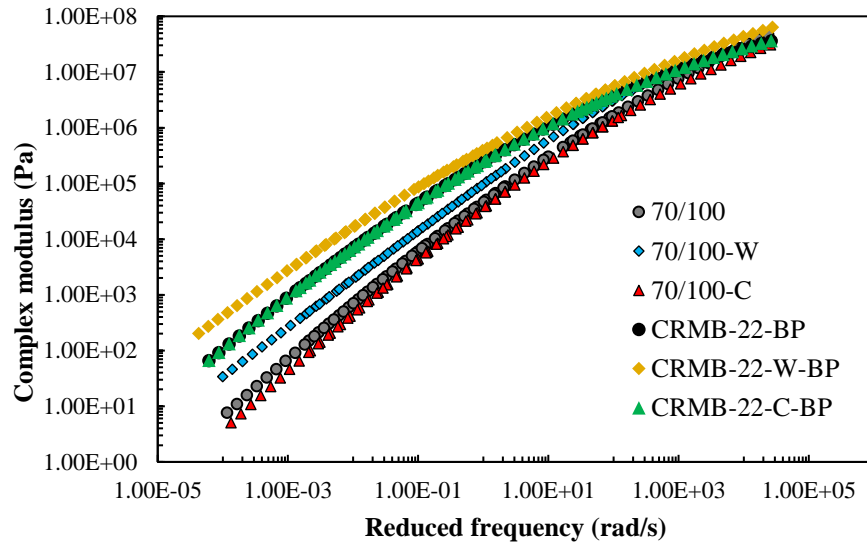


2

(b)

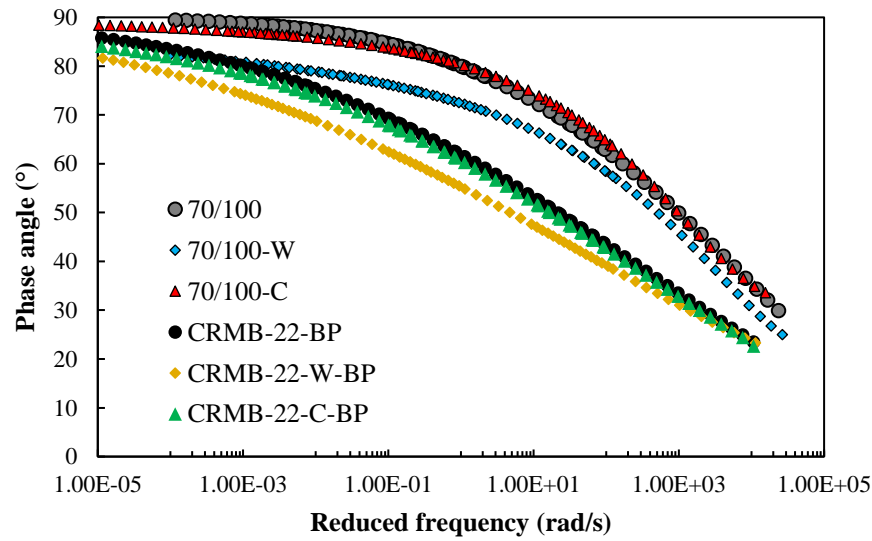
3 **Figure 10.** Viscoelastic master curves of bitumen and rubber phases: (a) complex modulus and (b) phase
4 angle.

5



1

(a)



2

(b)

3 **Figure 11.** Viscoelastic master curves of bitumen phases containing warm-mix additives: (a) complex
4 modulus and (b) phase angle.

5